

## BEHAVIOR OF FLAMMABLE GAS BUBBLES IN HANFORD HIGH-LEVEL WASTE

P. A. Gauglitz, G. Terrones, D. P. Mendoza, C. L. Aardahl  
Pacific Northwest National Laboratory  
Richland Washington 99352

### ABSTRACT

The Hanford Site has 177 underground waste storage tanks that are known to retain and release bubbles composed of flammable gases. Characterizing and understanding the behavior of these bubbles is important for the safety issues associated with the flammable gases. The retained bubbles respond to small barometric pressure changes in a complex manner, but careful analysis yields information on the volume of retained gas and the interactions of the waste and the bubbles. To investigate this behavior theoretically and experimentally, we have considered the effects of external pressure fluctuations on the deformation history of bubbles imbedded in a compressible elastic-plastic soft solid. For periodic pressure fluctuations, closed-form solutions have been obtained in the case of a single bubble in media of infinite and finite extent. In these analyses, the amplitude of the pressure variation was considered to be sufficiently high that the von Mises yield criterion was satisfied in a finite region in the vicinity of the bubble boundary. It was assumed that within the medium there was no stress relaxation following plastic deformation. Therefore, residual stresses were taken into account for every external compression and decompression excursion. Results show the occurrence of hysteresis of the bubble volume as a function of pressure fluctuations. Experiments have been conducted with single and multiple bubbles embedded in soft solid simulants of varying yield strengths. In these experiments, hysteresis has been observed between the externally controlled pressure and the volume expansion of the simulant.

### INTRODUCTION

The Hanford Site has 177 underground storage tanks containing wastes that are complex mixtures of radioactive and chemical products. Some of these wastes are known to generate and retain bubbles of flammable gases that contain hydrogen, ammonia, and the oxidizer, nitrous oxide. Because these gases are flammable and have the potential to be released rapidly, the volume of retained gas in each tank must be determined to establish the flammability hazard.

Previous studies on flammable gas bubble-laden radioactive sludge waste in some storage tanks at the Hanford Site have established that 1) the tank waste level responds to barometric pressure changes, 2) the compressibility of retained bubbles accounts for the level changes, and 3) the volume of retained gas can be estimated from the measured waste level and barometric pressure changes. Because the retained gas is typically a flammable mixture of hydrogen, ammonia, and nitrous oxide, determination of the retained gas volume is a critical component of establishing the safety hazard of the tanks.

Accurate determination of retained gas from waste level and barometric pressure data can only be obtained once the interactions between the gas bubbles and the rheologically complex waste are well understood. Elucidation of the interactions between bubbles and tank waste surrogates

will contribute to the development of models for determining 1) gas content in Hanford tanks, 2) waste properties from level/pressure data, and 3) the effect of barometric pressure fluctuations on the slow release of bubbles. Furthermore, a methodology for determining the amount of retained gas is necessary because direct in situ measurements are impractical in several tanks and impossible in many single-shell tanks.

The response of retained bubbles to small barometric pressure fluctuations is expected to induce a slow upward migration of the bubbles, and the subsequent release of these bubbles may play a crucial role in establishing the volume of retained flammable gases in Hanford waste tanks. While gas-bubble release mechanisms have been the focus of other recent studies, a mechanistic understanding of very slow bubble migration is absent.

Through the interaction of retained gas bubbles with the waste, the response of the waste level to barometric pressure changes may also provide information on the waste physical properties such as shear strength. Figure 1 shows that the level/pressure relationships for a specific tank during a large weather event. The arrows show the direction of the pressure change from the beginning of the event to the end. The level measurements exhibit hysteresis, and this hysteresis is thought to stem from the interaction of bubbles with the waste (1). A thorough understanding of the mechanics of bubbles in waste materials is needed to extract the physical property information. Currently, the material properties in nearly all of the tanks are unknown, largely because of the difficulty and cost of sampling the tanks and testing the material directly. Material properties are important to many proposed and ongoing tank operations such as waste mobilization and saltwell pumping.

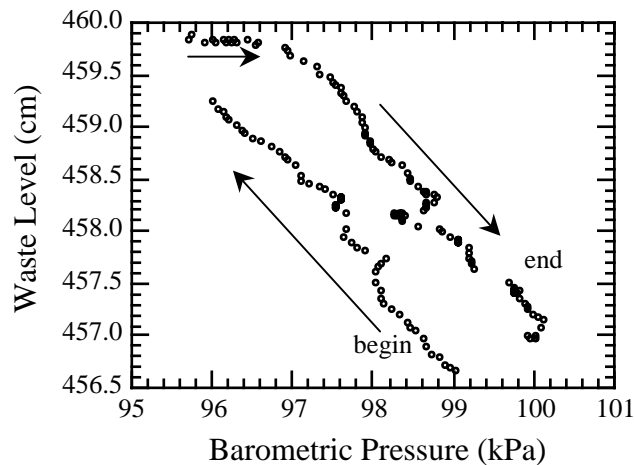


**Fig. 1.** Level/pressure hysteresis in radioactive sludge (1).

In this paper, we focus on the development of a model and related experimental testing for how bubbles interact with a soft solid representing the waste. The specific problem we study is of a bubble periodically compressing and expanding due to external pressure changes.

## SINGLE BUBBLE MATHEMATICAL MODEL

In this section, the theoretical analysis of the deformation of a single bubble in a compressible elastoplastic isotropic medium under external pressure fluctuations is briefly described. The general situation is considered in which the external pressure fluctuations are large enough to produce plastic zones during compression and reversed plastic zones during decompression. It is assumed that the rate of change of the pressure variations acting on the medium is sufficiently small that the inertial or dynamic effects become negligible. Under the condition of radial quasi-static expansion and contraction of the bubble, the equilibrium and compatibility equations are used to determine the state of elastic stress and strain within the medium. To determine the plastic stresses, the equations of equilibrium and the yield criterion must be satisfied. Yield is assumed to occur in the continuum according to the von Mises criterion.

Because of the symmetry of the problem, the only non-vanishing component of the displacement vector is in the radial direction. In addition, the state of stress in the angular directions is isotropic. Furthermore, the directions of the principal stresses correspond to those of the coordinate system. This implies that the radial and angular strains in the plastic regions can be represented by their corresponding logarithmic strains because the principal stresses coincide with the coordinate axis (2).

With the above assumptions and the simplifications due to spherical symmetry, the governing equations for the stresses and strains in the elastic region are

$$\text{Eq. 1} \quad \begin{bmatrix} \nu & \nu-1 \\ 1 & 0 \end{bmatrix} \frac{d}{dr} \begin{Bmatrix} \sigma_r \\ \sigma_\theta \end{Bmatrix} + \frac{1}{r} \begin{bmatrix} \nu+1 & -\nu-1 \\ 2 & -2 \end{bmatrix} \begin{Bmatrix} \sigma_r \\ \sigma_\theta \end{Bmatrix} = 0$$

$$\text{Eq. 2} \quad \begin{Bmatrix} \epsilon \dot{Y}_r \\ \epsilon \dot{Y}_\theta \end{Bmatrix} = \frac{1}{E} \begin{bmatrix} 1 & -2\nu \\ -\nu & 1-\nu \end{bmatrix} \begin{Bmatrix} \sigma \dot{Y}_r \\ \sigma \dot{Y}_\theta \end{Bmatrix}$$

where  $r$  is the radial coordinate,  $\sigma_r$  and  $\sigma_\theta (= \sigma_\phi)$  are the radial and angular stresses,  $\nu$  is the Poisson ratio,  $\epsilon Y_r$  and  $\epsilon Y_\theta$  are the radial and angular strain rates, and  $E$  is the Young's modulus of elasticity. The initial and boundary conditions for the elastic problem in a medium of infinite extent are

$$\text{Eq. 3} \quad \epsilon_r(r; 0) = \epsilon_\theta(r; 0) = 0, \quad \sigma_r(r; 0) = \sigma_\theta(r; 0) = -p_o$$

$$\text{Eq. 4} \quad \sigma_r(a; t) = -p_o \left( \frac{a_o}{a} \right)^3, \quad \sigma_r(\infty; t) = -p_o + p_A \sin\left( \frac{2\pi t}{T} \right)$$

where  $a_o$  is the initial bubble radius;  $a$  is the current radius, which is an unknown function of the external pressure; and the external pressure exerted on the medium is periodically varied in time  $t$  with a period  $T$ . When the outer boundary is finite, the number of equations for the elastic and plastic deformations is twice that of infinite media. At each pressure sweep, the expressions for these deformations are obtained analytically but solved numerically because they involve

nonlinear implicit functions. The elastoplastic solution in a medium of finite extent can be found in Terrones and Gauglitz (3).

The conditions given in Eq. 4 correspond to realistic boundary conditions because the internal bubble pressure is implicitly coupled to the bubble radius, and the pressure fluctuations are externally applied to the medium. It was assumed that the bubbles contain an ideal gas and the compression/expansion of the bubble is isothermal. During any given pressure sweep, the continuum in general comprises a finite plastic region and an infinite elastic region. As time evolves, the alternate compression and decompression cycles create states of residual stress that constitute the initial conditions for the subsequent pressure sweep. For a given pressure sweep, two different sets of equations are solved to determine the plastic and elastic states of stress and strain. Two additional boundary conditions are introduced: the yield criterion is satisfied at the plastic-elastic boundary (which is not known a priori), and the stresses are continuous across this boundary.

When a finite plastic zone is formed, the equations for the stresses and the finite displacements are

$$\text{Eq. 5} \quad \begin{bmatrix} r & 0 \\ 0 & 0 \end{bmatrix} \frac{d}{dr} \begin{Bmatrix} \sigma_r \\ \sigma_\theta \end{Bmatrix} + \begin{bmatrix} 2 & -2 \\ (-1)^n & (-1)^{n+1} \end{bmatrix} \begin{Bmatrix} \sigma_r \\ \sigma_\theta \end{Bmatrix} = \begin{Bmatrix} 0 \\ \sigma_y \end{Bmatrix}$$

$$\text{Eq. 6} \quad \ln \left( \frac{r^2 dr}{r_0^2 dr_0} \right) = \frac{1-2\nu}{E} (\sigma_r + 2\sigma_\theta) + \left[ \varepsilon_r + 2\varepsilon_\theta - \frac{1-2\nu}{E} (\sigma_r + 2\sigma_\theta) \right] \Big|_{t=\text{Onset of Yield}}$$

$$\text{Eq. 7} \quad \varepsilon_r = \ln \left( \frac{dr}{dr_0} \right), \quad \varepsilon_\theta = \ln \left( \frac{r}{r_0} \right)$$

where n is 0 or 1 during external compression or decompression, respectively; r is the current radial coordinate; r<sub>0</sub> is the original radial coordinate; and σ<sub>y</sub> is the yield stress of the material in pure tension. The initial conditions for the plastic displacements are obtained from the state of stress-strain at the onset of yield. This is calculated by evaluating the elastic solution at the critical pressure (above which there is plastic yield). For the combined plastic and elastic problems, the boundary conditions are

$$\text{Eq. 8} \quad \sigma_r^p(a) = -p \left( \frac{a_0}{a} \right)^3, \quad \sigma_r^e(b) - \sigma_\theta^e(b) = (-1)^n \sigma_y$$

$$\text{Eq. 9} \quad \sigma_r^p(b) = \sigma_r^e(b) \quad \sigma_\theta^p(b) = \sigma_\theta^e(b)$$

$$\text{Eq. 10} \quad \sigma_r^e(\infty) = -p_o + p_A \sin \left( \frac{2\pi t}{T} \right)$$

where the superscripts p and e denote plastic and elastic solutions, respectively. After reaching the maximum decompression, the external pressure is increased and compression begins by

retracing the same pressure values followed by the previous sweep. However, at the same pressure value, the state of stress during compression is different from that of decompression because of the presence of residual stresses. Residual stresses are the sum of the original state of stress (before the beginning of compression) and the elastic stresses originating from the departure of the state of stress from the maximum decompression point (4,5). Initially, compression causes a state of elastic stress that is followed by the formation of a reversed plastic zone. During this pressure sweep, the elastic and plastic equations are solved by taking into account that the extent of the new plastic zone is different from that obtained during decompression and that the bubble radius has changed because of an irrecoverable plastic displacement. For a detailed account of this procedure and its generalization to an arbitrary number of pressure sweeps, refer to Terrones and Gauglitz (6).

Figures 2a and 2b show the prediction of changes in the bubble radius as the pressure is periodically varied. During decompression, the rate of increase in the bubble radius markedly increases after the formation of a plastic zone. From the beginning of compression, the medium loads elastically to a critical pressure below which the material loads plastically until the maximum compression point is reached. This behavior repeats during the last decompression sweep. Notice the difference between the bubble radius at the start and at the end of the pressure cycle (the original radius is not recovered). If the bubble were subjected to a hydrostatic state of compression or expansion, the dependence of bubble radius on time-periodic pressure would produce a single curve. Figure 2a shows that increasing the waste strength causes an increasing hysteresis in the relationship between bubble radius and pressure. This occurs because the waste, which is a soft solid, resists the expansion and compression of the bubble. Figure 2b shows that the hysteresis depends on Young's Modulus as well.

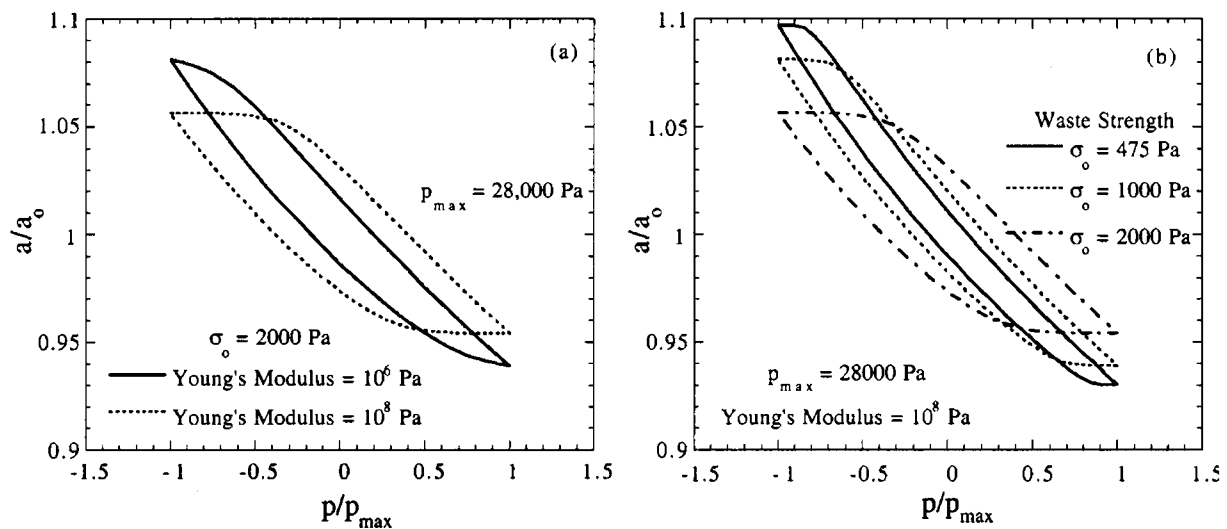


**Fig. 2.** The role of waste physical properties on the hysteresis during expansion and compression of a bubble: a) effect of yield stress, b) effect of modulus of elasticity.

## EXPERIMENTAL METHOD AND MATERIALS

The test stand for examining single bubble behavior is depicted in Figure 3. The single bubble cell comprises a glass vessel mounted beneath a glass capillary. A capillary is employed to magnify the minute volume changes of the bubble into measurable level changes in the capillary. The pressure above the capillary is regulated using a controller and a vacuum control valve. Video cameras are used to record bubble shape and level changes in the capillary tube. The position of the meniscus in the capillary is determined by image analysis to obtain the level as a function of pressure. Video recording equipment is available to provide a pictorial record for examination of bubbles and/or level changes subsequent to experiments. System controls and image analysis are performed with National Instruments hardware and LabView software.

A variety of particulate-liquid systems have been employed. There are two systems that show promise, but each has limitations. The first is carboxyl polymethylene (Carbopol)-water, which is a polymer solution rather than two-phase, and the second is a silica-oil system. The Carbopol solutions are crystal clear and have the desired yielding behavior (50 to 2000 Pa strength), but the Young's modulus is low, which results in accentuated elastic behavior. The oil-silica system has all the desirable properties, but air is reasonably soluble in the mineral oil that is needed to obtain a clear dispersion. This results in volume changes due to gas transfer across the bubble-simulant interface.

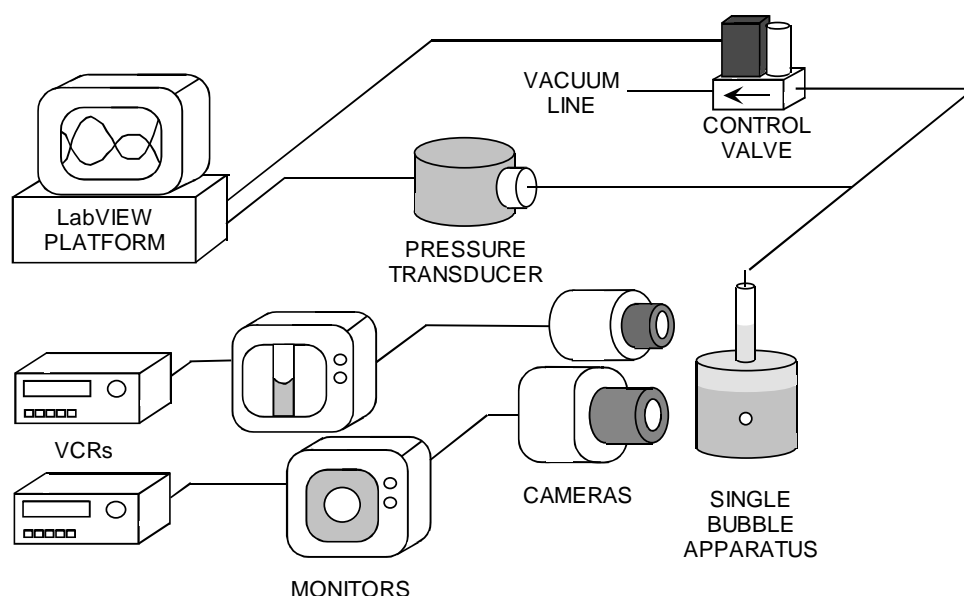


**Fig. 3.** Apparatus for pressure and bubble volume measurements for single bubbles.

## EXPERIMENTAL RESULTS

The best representation to tank waste behavior has been observed with the silica-oil system. This is likely due to the thixotropic nature of the Cab-O-Sil M5 silica (Cabot Corp.) that was used. Hydrogen bonding between the particles in the suspension mimics the brittle behavior observed in tank sludges, whereas the aqueous-based Carbopol simulant shows significant elastic creep uncharacteristic of real wastes. Figure 4 shows the effect of a positive step change in pressure on

the two simulants studied thus far. Notice that the water-based simulant shows creep during the first 30 minutes, while the oil-based system shows significant gas dissolution hours after the step change. When the pressure is raised above the oil-based simulant, the pressure in the gas bubbles rises. Because the solubility of air is substantial in mineral oil, some of the gas within the bubble partitions into the liquid over time. In general, hydrogen has a low solubility in the actual tank waste, and partitioning of hydrogen across the surface of bubbles is not expected. However, many of the tanks have significant amounts of ammonia in the trapped gas bubbles, and ammonia is soluble in tank waste. Therefore, we believe that the oil-based simulant may be valuable for further examination of gas-uptake and gas-evolution phenomena, particularly in experiments involving pressure cycles characteristic of atmospheric pressure fluctuations.

In order to examine the effect of waste strength on the change in bubble volume with pressure, the gas exchange between the bubble and suspension must be minimized. Therefore, the pressure above the capillary was cycled over a short time scale. Figure 5 shows the response of two silica-oil simulants to a sinusoidal 10-minute pressure cycle with an amplitude of 10 minutes. Here, bubble volume – pressure change data have been transformed to dimensionless form. Both data sets show hysteresis, but the stronger material shows a larger degree of hysteresis. This trend is in agreement with the model prediction shown in Figure 2.

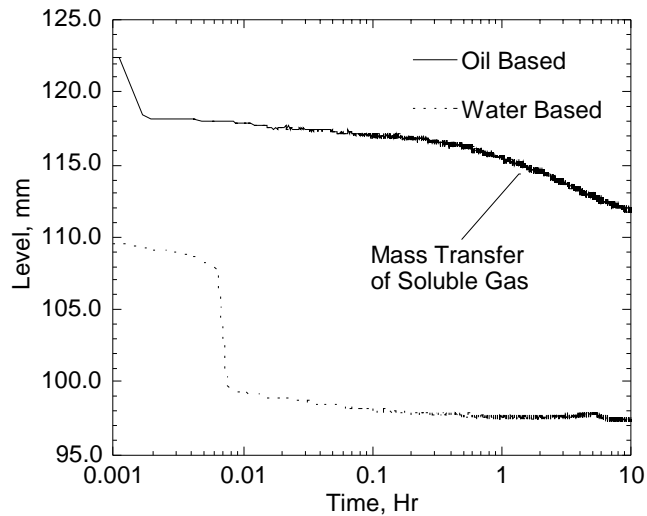


**Fig. 4.** Step changes in pressure show the effects of mass transfer across the bubble surface.

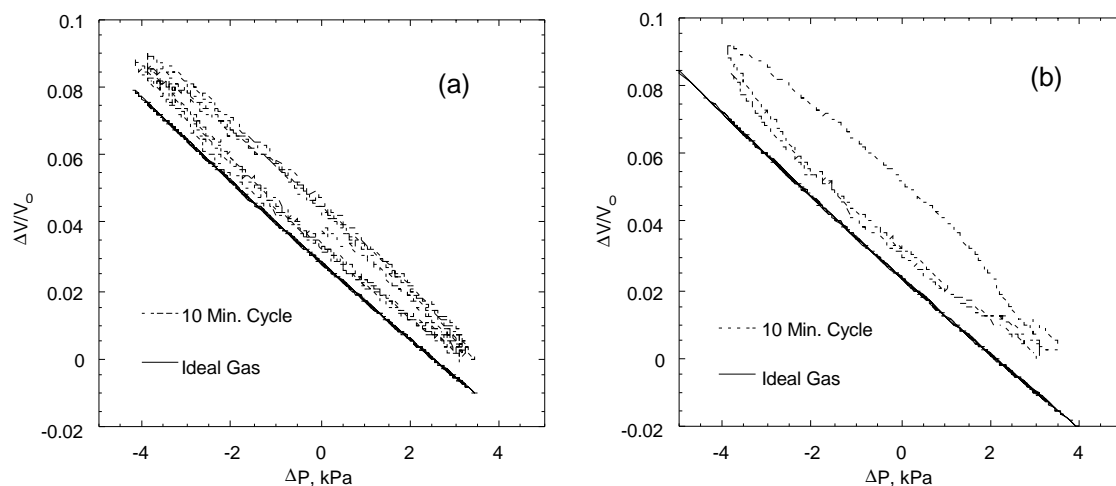


**Fig. 5.** Bubble volume-pressure change data plotted in dimensionless form for two oil-silica simulants: (a) 5% Cab-O-Sil M5 in mineral oil (20 Pa), and (b) 6.5% Cab-O-Sil M5 in mineral oil (200 Pa).

## DISCUSSION AND CONCLUSIONS

Modeling of the bubble/waste interactions from a solid mechanics approach was initiated with a theoretical study to understand the effects that smooth external pressure fluctuations have on the deformation history of a single bubble imbedded in a compressible elastic-perfectly plastic isotropic medium of infinite extent. The problem was approached by solving an outer elastic and an inner plastic problem for each compression and decompression sweep of the pressure cycle, then matching the deformations and stresses at the elastic-plastic boundary. Finite deformations were used to determine the displacements in plastic regions. The general case in which forward and reverse yield zones alternate with each pressure cycle was considered. The mathematical model was capable of predicting a hysteretic behavior between the volumetric and pressure fluctuations. The hysteresis loop can be traced to the formation of forward and reverse yield regions during compression and decompression.

The experimental studies focused on quantifying the effect of small pressure changes on the volume of a single, nearly spherical bubble in a waste simulant. In experiments with single bubbles embedded in soft solid simulants (19-nm fumed silica particles dispersed in light mineral oil) of varying yield strengths, hysteresis was observed between the externally controlled pressure and the volume expansion of the simulant. The trend in degree of hysteresis is consistent with model predictions of materials with different yield stresses though the single bubble experiments show less of an effect than predicted. Hysteresis of tank level with pressure changes, which is equivalent to hysteresis in bubble volume changes, has been observed in some Hanford tank wastes (which are known to have yield stress) (1). Unlike the data from the Hanford tanks, the single bubble data show rounded corners at the bottom and top of the cycle. The model developed under this program suggests that the reason for such smoothing is a lower Young's modulus of elasticity for the simulants versus actual tank waste. In future studies,



## WM'00 Conference, February 27 – March 2, 2000, Tucson, AZ

detailed rheological measurements will be made to determine the Young's modulus of selected simulants, allowing for a quantitative comparison of the model with the experimental results.

### REFERENCES

1. P.D. Whitney, P.A. Meyer, N.E. Wilkins, N.E. Miller, F. Gao, and A.G. Wood, *Flammable Gas Data Evaluation Progress Report*, PNNL-11373, Pacific Northwest National Laboratory Report, Richland, Washington (1996)
2. J. Lubliner, *Plasticity Theory*, Macmillan Publishing Company, New York (1990)
3. G. Terrones and P.A. Gauglitz, "Deformation Path of a Spherical Gas Bubble Soluble in an Elastoplastic Medium," to be submitted to *Journal of Applied Physics* (2000-a)
4. P. Chadwick, "The Quasi-Static Expansion of a Spherical Cavity in Metals and Ideal Soils," *Quart. J. Mech. Appl. Math.*, **12**, pp. 52-71 (1959)
5. H.G. Hopkins, "Dynamic Expansion of Spherical Cavities in Metals," in *Progress in Solid Mechanics*, Snedon, I.N., and Hill, R. (eds.), North-Holland, Amsterdam, **1**, pp. 85-164 (1960)
6. G. Terrones and P.A. Gauglitz, "Effect of Periodic External Pressure Fluctuations on the Volumetric Hysteresis Behavior of a Spherical Bubble in an Elastoplastic Medium," to be submitted to *Journal of Applied Mechanics* (2000-b)